

International Journal of Pharmacy and Industrial Research (IJPIR)

IJPIR | Vol.14 | Issue 4 | Oct - Dec -2024 www.ijpir.com

DOI: https://doi.org/10.61096/ijpir.v14.iss4.2024.630-637

ISSN: 2231-3656 Print: 2231-3648

Research

Development of Novel Nano-Elastic Carriers for Trametinib Delivery in Melanoma Treatment

Chokkarapu Suryanarayana¹, Ankit Singh¹, Ananda Kumar Chettupalli*²,

- ¹Research scholar, Department of Pharmaceutical sciences, Shri Jagdish Prasad Jhabarmal Tibrewala University Chudela Jhunjhunu Rajasthan- 333001.
- ¹Department of Pharmaceutical sciences, Shri Jagdish Prasad Jhabarmal Tibrewala University Chudela Jhunjhunu Rajasthan- 333001.
- *.2Department of Pharmaceutical sciences, School of Medical and Allied Sciences, Galgotias University, Greater Noida, UP-203201.
- *Author for Correspondence: Ananda Kumar Chettupalli Email: anandphd88@gmail.com

Abstract

Check for updates

Published on: 22 Dec 2024

Published by: DrSriram Publications

2024 All rights reserved.



<u>Creative Commons</u>
<u>Attribution 4.0 International</u>
<u>License.</u>

regulatory kinase (ERK), is a clinically licensed targeted therapy by the Food and Drug Administration (FDA) for treating refractory malignancies with BRAF-V600E gene mutations, such as melanoma and advanced lung adenocarcinoma. Nonetheless, the commercial Tr is constrained in clinical applications due to its low solubility, absence of bio-targeting, and a significant concern is its propensity to generate multidrug resistance in tumour cells. The produced formulations demonstrated that the optimal results were achieved with a high concentration of the mucoadhesive polymer chitosan (0.5 and 1% w/v). The chitosan-coated bilosomes (TM-CBLs) were subsequently assessed for surface morphology, antioxidant activity, and antibacterial activity. The synthesised TM-BLs exhibited a nanometric size ranging from 185.34±5.28 nm (BS3) to 295.31±6.31 nm (BS5), a polydispersity index of less than 0.5, a negative zeta potential of -10.74±1.06 mV and -21.54±1.42 mV, and an improved encapsulation efficiency of 56.49±0.16% to 80.27±0.64%. According to these findings, the chosen formulation (BS2) was subsequently coated with chitosan, resulting in a significant increase in vesicle size (268.49±2.31nm), a positive zeta potential (17.36±0.52 mV), enhanced encapsulation efficiency (87.35 \pm 0.26%), and increased drug release (69.37 \pm 1.34%). The TM-CBLs formulation exhibited markedly improved permeability and mucoadhesion (p < 0.05) relative to the BS2 formulation, attributable to the inclusion of chitosan as a mucoadhesive polymer. The evaluation of antibacterial and antioxidant activity demonstrated superior benefits regarding the zone of

Trametinib (TM), an inhibitor of mitogen-activated extracellular signal-

Keywords: Trametinib, Melanoma, Chitosan, Bilosomes, anti-oxidant activity, antimicrobial activity.

inhibition. The study concludes that TM-BLs may serve as a superior alternative to

traditional delivery techniques.

INTRODUCTION

The unchecked growth of melanocytes characterises melanoma, one of the most deadly types of skin cancer. Melanoma treatment still faces formidable obstacles, such as limited medication absorption, systemic toxicity, and multidrug resistance, despite progress in cancer therapy. By blocking the mitogen-activated protein kinase (MAPK) pathway, the powerful MEK inhibitor trametinib has demonstrated outstanding effectiveness in targeting melanoma. Unfortunately, its fast metabolic breakdown, low permeability, and poor water solubility restrict its therapeutic use. 1,2

A new and potentially useful drug delivery technology, nano-elastic carriers, have arisen to circumvent these restrictions. Improved medication absorption and targeted distribution to melanoma cells are made possible by these carriers' exceptional penetration, flexibility, and stability. Examples of such carriers are ethosomes, elastic liposomes, and transfersomes. In order to make melanoma treatment more effective, we want to encapsulate Trametinib in nano-elastic carriers so that the medicine is more bioavailable, penetrates the skin better, and has less systemic side effects.³

This work assesses the physicochemical properties, in vitro drug release, skin penetration, and in vivo therapeutic efficacy of nano-elastic carriers loaded with Trametinib. The carriers are formulated, characterised, and evaluated. Improving melanoma management and paving the road for precision medicine driven by nanotechnology could be possible with the development of this enhanced drug delivery system.⁴

MATERIALS AND METHOD

Materials

TM was obtained as a gift simple from Hetero laboratory, Hyderabad, Telangana, India. Sodium glycocholate dried (SGC dried) extra pure, M.W.487.60 was purchased from S.G enterprises, New Delhi, India and dialysis sac (MWCO: 12000 Da, average flat width was 2.5 mm, a capacity of 60 mL/ft, 16 mm of diameter) was procured from Sigma Aldrich, India. Cholesterol was purchased from Thermo Fisher Scientific, India. Chloroform, span 60, tween 60, and diethyl ether were purchased from SD fine chemicals, Mumbai, India. Mannitol M.W. 182.17 g/mol, was purchased from SD fine chemicals, Mumbai, India). All other chemicals and reagents used in the study were of analytical grade.

Preparation of TM loaded BLs

Formulation of TM-loaded BLs were formulated using the thin film hydration technique described by Waglewska et al. (Citation 2020). Briefly, 10 mg TM, cholesterol (CH, 7.5mg), and bile salt 10mg and surfactant 50 mg were solubilized by the use of an ultrasonic bath sonicator (Ultrasonic bath sonicator, Model SH 150-41; USA) for 10 min in 10 mL chloroform in a round bottom flask. The obtained organic solution was subjected to evaporation at 40 °C under reduced pressure using a rotary evaporator (Rotavapor, Heidolph VV 2000; Heidolph Instruments, Kehlheim, Germany) for 30 min till obtaining a dry and thin film. The film formed by evaporation was left overnight to ensure complete evaporation of residual organic and then rehydrated in 10 ml distilled water containing STC. The resultant dispersion was magnetically stirred for 2 h to generate a dispersion of TM-BLs. To reduce particle size (PS) of the obtained dispersion of BLs, the dispersion was ultrasonicated for 5 min (Bandelin, Berlin, Germany). The prepared TM-BLs dispersion was kept at 4 °C until use.

Drug/Excipients	BS-1	BS-2	BS-3	BS-4	BS-5	BS-6	CBS-2	CBS-2
Trametinib (mg)	10	10	10	10	10	10	10	10
SDC (mg)	20	30	40				20	20
STC (mg)	-	-	-	20	30	40	-	-
Tween 80 (mg)	10	20	30				40	50
Cremophor EL(mg)	-	-	-	10	20	30	-	-
Cholesterol (mg)	5	5	5	5	5	5	5	5
Chloroform (mg)	5	5	5	5	5	5	5	5
Chitosan (%w/v)	-	-	-	-	-	-	0.5	1

Table 1: Formulation of Drugs loaded Novel nano elastic vesicles (Bilosomes)

Optimization of bilosomes

The selection of optimal formulation for further investigations was done with the intention to have optimum vesicle size, minimum PDI, and maximum drug entrapment. To achieve the goal, the influence of variables on particle size, PDI, and %EE was analysed.

Physicochemical characterization Particle size, PDI, and zeta potential

The particle size of bilosomes (TM-BS) was specified by measuring Brownian motions of nanocarriers using dynamic light scattering (DLS) technique by Zetasizer Nano Series from Malvern Instruments (Worcestershire, UK; DTS software) with an angle of incidence of light equal to 173° . Three runs with at least ten measurements in disposable polystyrene cuvettes were performed at 25 °C and were reported as Z-average (Z-Ave) in conjunction with polydispersity index (PdI). The nanobilosomes' surface electric charge (ζ -potential) was determined using the Smoluchowski equation, using the electrophoretic mobility technique and monitoring the movement of the particles in an electric field. The measurements were conducted in a folded capillary zeta cell at 25 °C using the same apparatus as above (three consecutive instrument runs, with at least twenty measurements). Z-Ave, PdI, and ζ -potential measurements were performed again after a suitable incubation time (14 and 30 days) at 4 °C to check the system's stability.⁵

Entrapment efficiency percentage (EE%)

Entrapment efficiency was estimated by the direct method. TM-BLs were sonicated in ethanol for 10 min and filtered through a syringe filter (pore size: $0.4\,\mu m$) (Millex-LG, Millipore Co., USA). The amount of TM entrapped within BLs was estimated using a Shimadzu UV spectrophotometer (2401/PC Japan) at 245 nm (El-Nassan, Citation2014; Van Nong et al., Citation2016) The EE% was calculated using the following equation (Equation Equation 1):

%EE =
$$\frac{Amount\ of\ encapsulated\ drug}{Total\ amount\ of\ drug} X100$$

Scanning electron microscope

A scanning electron microscope was used to assess the morphological features of the optimized bilosomal formulations and to evaluate the shape of the formed system. Before visualization, freshly prepared samples (1 mg/mL) were diluted with filtered deionized water (1:50) and subjected to bath sonication for 5 min at room temperature. A sample drop was placed onto a carbon-coated copper grid and stained using an aqueous solution of 1% uranyl acetate for 30 s then left to dry out. Afterwards, the stained film was visualized using SEM (SEM, JEM-2100F; JEOL, Tokyo, Japan).

In-vitro drug release and release kinetics

In-vitro drug release was measured using the dialysis bag diffusion technique. Briefly, a sample of BLs dispersion containing 10 mg TM was placed in the cellulose dialysis bag and submerged in up to 15 ml of 0.1 M PBS (pH 6.8), 0.1% tween 20 was added to maintain sink condition. At predetermined time intervals, 2-ml samples of the receiver medium were withdrawn and replaced by an equivalent fresh medium volume to maintain both constant volume and sink conditions. The amount of TM in receiver medium samples was determined by UV spectrophotometry at 245 nm (Abbas et al., Citation2018; El-Telbany et al., Citation2021). Release data from CU, PIP suspensions, and different BLs formulations were fitted to zero, first-order, and Higuchi equations using DD solver software.

In-vitro anti-oxidant study

DPPH radical scavenging method

In-vitro antioxidant activity of TM and TM-BS was measured by the DPPH free radical scavenging method (Clarke et al., Citation2013). The various concentrations of TM and TM-BS ($10-150\,\mu g/ml$) from stock solution ($1\,mg/ml$) were prepared in methanol. The 0.1 M of DPPH was prepared in methanol and stored at 4° C until used. For the completion of the reaction, $500\,\mu L$ of each sample was mixed with $100\,\mu L$ of DPPH solution and stood for 1 h in a dark place. When the reaction was completed, the color changed to colorless from violet, indicating the scavenging activity. The absorbance was measured by UV-spectrophotometry at 571 nm. A blank (butylated hydroxytoluene, BTH) was taken as a control. The percent antioxidant activity of the tested sample was calculated by the following EquationEq. 6

% Antioxidant activity =
$$\frac{Abs\ Control - Abs\ of\ test\ sample}{Abs\ control} X100$$

ABTS radical scavenging method

The study was performed as per the previously described method with a small modification 7 (Chaves et al., 2020). The various concentrations of TM and TM-BS (10–150 µg/ml) were prepared and 0.1 ml of each dispersion was mixed with 3.9 ml of ABTS solution and vortexed. The mixture was incubated for 30 min in a dark place and analyzed by UV-Vis spectrophotometry at 734 nm. The BTH solution is taken as a blank for comparative analysis. The percentage of scavenging activity was calculated by the following formula 10.89

% Antioxidant activity =
$$\frac{Abs\ Control - Abs\ of\ test\ sample}{Abs\ Control} X100$$

Antimicrobial study

The antimicrobial evaluation of pure TM and TM-BS was done on Staphylococcus aureus (S. aureus, gram-positive) and Escherichia coli (E. coli, gram-negative) microbial strains using the cub plate method. The culture was grown in nutrient broth media equivalent to 5×10^6 CFU/ml bacterial load. The nutrient agar medium was prepared and sterilized at 121^{0} C in an autoclave. The 0.5 ml (diluted) of microbial strain was mixed with liquid nutrient agar media and transferred to a sterile Petri plate under aseptic conditions and allowed to stand for solidification. After solidification, the 6 mm cup was made using a sterile stainless-steel borer. The test sample (TM and TM-BS) was filled into each cup and stood for 2 h for absorption of the test sample. Then a Petri plate was placed into the incubator in an inverted positin at 37^{0} C for 24 h. The zone of inhibition (ZOI) was then measured using a graduated scale. ¹⁰

Statistical analysis

Experimental design software (version 8.0.6) was used for the optimization of the formulation. The value was represented in mean \pm SD. GraphPad (InStat, CA, USA) was used for statistical analysis. One-way ANOVA and Tukey-Karman multiple comparison tests were used for data analysis. Significant differences were taken at P < .05.

RESULTS AND DISCUSSIONS

TM-BLs were prepared by a thin film hydration method using cholesterol, sodium deoxy cholate (SDC) and sodium taurocholate (STC). The formation of TM-BLs was mainly attributed to electrostatic interaction between positively charged cholesterol and negatively charged BLs. The addition of positively charges to anionic BLs lead to changes in size and zeta potential. An increase in size may have been due to surface coating from cholesterol and the formation of double-layered vesicles. The prepared TM-BLs had nano-metric VS, low PDI, negative ZP and high EE. Based on these findings, the selected formulation (F2) was further coated with cholesterol (7.5 and 30 mg), and a marked increase in size and a negative zeta potential were observed (Table 2).

Fprmulation code	VS	EE	PDI	ZP	Drug Loading
BS-1	215.34±3.46	75.54 ± 0.35	0.115 ± 0.01	-16.58±1.02	68.35 ± 1.24
BS-2	185.85±6.91	82.27±0.64	0.129 ± 0.04	-24.54±1.42	86.58±2.56
BS-3	164.34±5.28	69.34±0.28	0.248 ± 0.03	-19.69±1.03	75.42±3.28
BS-4	259.41±4.72	52.49±0.16	0.352 ± 0.05	-12.74±1.06	58.34±2.49
BS-5	285.31±6.31	67.57±0.53	0.279 ± 0.01	-18.53±1.52	64.18±2.45
BS-6	264.58±5.34	73.31±0.28	0.386 ± 0.06	-19.84±1.48	66.59±1.06
CBS-1	268.49±2.31	84.36±0.45	0.442 ± 0.04	17936±0.52	89.35±0.26
CBS-2	352.74±3.65	92.24±1.36	0.466 ± 0.06	25.480.18	91.42±0.59

Table 2: Physicochemical characterization data of TM-BLs

Vesicle Characterization

The prepared TM-BLs were evaluated for VS, EE, PDI, drug loading and zeta potential (Table 2). A significant (p < 0.001) difference in the VS was found among TM-BLs. TM-BLs (BS1–BS6) showed mean sizes of 185.34±5.28 (BS3) to 295.31±6.31nm (BS5). The minimally-sized formulation F3 (185.34±5.28nm). We found a significant (p < 0.001) enhancement in size after coating with chotosan compared to formulation F2 (213.85±6.91 nm vs. 268.49 ± 3.02 nm). The chitosan concentration (0.5% or 1%) significantly (p < 0.001) affected the vesicle size. The literature reports that larger particles enter the lymphatic system, whereas particles under 500 nm in diameter use the endocytosis pathway for the transport of drugs [2]. In our study, TM-BLs and TM-CBLs had particle sizes below 500 nm. This size can also enhance drug absorption due to availability of a greater surface area. PDI value did not show any significant variation in the results (0.13 to 0.39). TM-BLs and TM-CBLs showed PDI values < 0.7 and considered as suitable delivery systems [25]. The surface charge on vesicle is very important for cellular interaction and uptake. A high negative zeta potential of the prepared TM-BLs indicates superior stability. The nano-sized TM-BLs showed values between -10.74±1.06 and -21.54±1.42 mV (±30 mV considered as stable) [26]. The values can be considered a distinguishing characteristic of TM-BLs. Flocculation exceeded repulsive forces [27]. The low ZP can be explained by the contribution of the lipids: the formation of negative charges in an aqueous environment. The surface of each particle was completely covered

with positively charged chitosan, and repulsion among the BLs thereby took place. ¹¹ A positive charge of chitosan easily binds with negatively charged intestinal mucin and will help to increase drug properties. ¹²

Entrapment Efficiency (EE)

The prepared TM-BLs was assessed for amount of TM entrapped in the bilosomes (Table 2). A significant (p < 0.001) differences in the EE (56.49 ± 0.16 to $80.27\pm0.64\%$) were observed due to difference in BLs composition. The sample (BS4) showed the minimum EE of 56.49 ± 0.16 %, having the composition STC (10 mg) and cremophre EL (40 mg). Formulation BS2 prepared with SDC (10 mg) and Tween 80 (50 mg) had the maximum encapsulation efficiency ($80.27\pm0.64\%$). EE improved with an enhancement in the concentration of bile salts/surfactant (individually or together). From the results, it was observed that T80 or SDC alone did not significantly increase the EE. The blend of SDC and T80 (1:1) significantly (p < 0.05) enhanced EE compared to T80 or SDC alone. At high concentration, it could help to form mixed micelle and contribute to enhanced solubility in the dispersion medium [30,31]. The formulation (BS2) further coated with chitosan (0.5% w/v and 1% w/v). A non-significant difference in the EE was observed in the TM-CBLs (CBS-1, CBS-2). There was a slight alteration in the EE was also found between CBS-1 ($89.36\pm0.45\%$) and CBS-2 ($91.24\pm1.36\%$). Chitosan formed surface coating over the lipid bilayer of liposomes and prevented the leakage of the drug [32]. The formulation CBS-2 showed slightly high EE due to the high concentration of chitosan (1%) as a coating polymer. The encapsulation of the drug depends upon the concentration of lipid and the concentration of polymer. The hydrophobic drug can easily entrap in the lipid bilayer.

Physicochemical characterization ■ VS 400 **EE** ■ PDI 350 - ZP 300 ■ Drug Loading 250 200 150 100 50 0 BS-5 BS-2 BS-3 BS-4 BS-6 CBS-1 CBS-2 -50

Fig 1: Physicochemical characterization data of TM-BLs

SEM Evaluation

The surface morphology of the prepared TM-BLs (optimized BS2) and TM-CBLs (CBS-1) showed non aggregated spherical structure (Figure). The outer surface was found to be smooth and thin layer of coating was observed. The samples (BS2, CBS-1) also evaluated for size distribution curve and the image showed size distribution between 200 to 45 nm (Figure). The distribution histograms are in close agreement with the results of SEM particle size image.

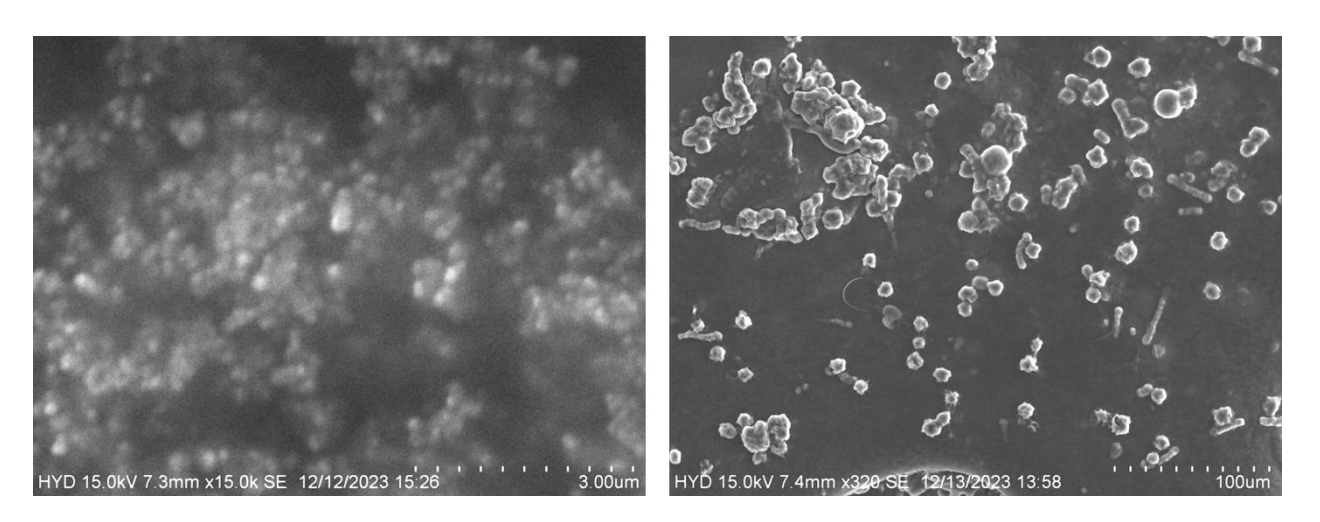


Fig 2: SEM images of Optimized TM-BLs (BS2) and TM-CBLs (CBS-1)

Drug Release (%)

The drug release of pure TM, TM-BLs and TM-CBLs were evaluated and the graph shown in Figure 3. The in vitro release data revealed higher TM release from TM-BLs (BS2) and TM-CBLs (CBS-1). The data revealed that drug efflux from the tested formulations was found to be a biphasic mechanism. In initial 2 h, a quick release was achieved and later the prolonged-release was achieved. TM-BLs (BS1-BS6) showed a higher drug release than the pure TM in the tested time period. The pure TM showed poor drug release (19.36 \pm 0.37) from the dialysis bag due to poor water solubility. TM-BLs showed significantly higher release: $42.61 \pm 0.62\%$ (BS3) to $74.39 \pm 0.58\%$ (BS2) (p < 0.05). The higher drug release by TM was due to nano-metric vesicle size and availability of more effective surface area. An increase in the surface area leads to an increase in contact points of the drug in dissolution medium. The presence of surfactant in BLs also helped to solubilize TM in dissolution media. Initially, a quick release occurred due to the availability of TM on the surfaces of the vesicles, and then slower release occurred. The slower drug release was due to encapsulated drug in inner core of BLs being released by diffusion and erosion or swelling of carrier. For TM-CBLs (CBS-1, CBS-2), the drug release was found to be slower than for TM-BLs. TM-CBLs (CBS-1) showed significantly slower release (56.34 ± 0.19 for 1 % chitosan and $63.52 \pm 0.85\%$ for 0.5% chitosan; p < 0.05) during the last period of the experiment. The presence of an extra layer of chitosan helped to retard the release which may behelpful for prolonging release in the body. The drug then needed to cross two layers to reach the release medium. The negative surfaces of the BLs were coated with chitosan via electrostatic interaction, reducing the release of TM.¹³

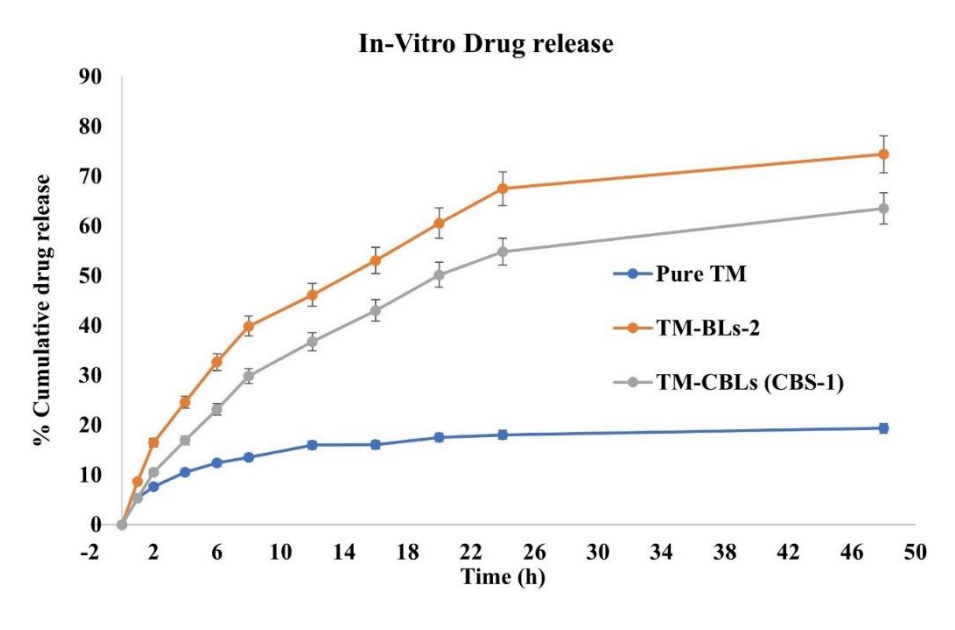


Fig 3: Release profiles of pure Trametinib (TM), TM-BLs (BS-2) and chitosan-coated TM-BLs (CBS-1). The data are shown as means \pm SDs (n = 3).

In-vitro anti-oxidant

TM-BLs were prepared by using cholesterol, SDC and Tween 80 in different concentrations. The prepared formulations showed nano-metric vesicle size, negative zeta potentials, low PDI and high EE. Then, the selected formulation (BS2) was coated with chitosan (0. 5, 1% w/v) to enhance its mucoadhesion. The chitosan-coated TM-CBLs (CBS-1 and CBS-2) were slightly larger, had a positive zeta potential, showed higher entrapent efficiency as well as provided slower drug release. The chitosan-coated bilosomes (CBS-1) showed significantly (p < 0.05) enhanced TM permeation and mucoadhesion. TM-BLs and TM-CBLs exhibited a greater antibacterial potential against E. coli than S. aureus than TM-dispersion. Finally, all of the findings suggest that TM-BLs could be a viable technique for the increment of TM efficacy against certain diseases. 14,15

CONCLUSTION

Our study demonstrates that the development of novel nano-elastic carriers for Trametinib delivery significantly enhances its solubility, stability, and bioavailability, overcoming the limitations of conventional formulations. The optimized bilosomal and chitosan-coated bilosomal formulations exhibited superior drug entrapment efficiency, sustained release profiles, and improved mucoadhesive properties. These results suggest that such advanced drug delivery systems hold great promise for improving Trametinib's therapeutic efficacy in melanoma treatment. Furthermore, the findings underscore the potential of nanotechnology-driven approaches in targeted drug delivery, reducing systemic toxicity while enhancing site-specific action. Future research should focus on in vivo evaluations, clinical translational studies, and further optimization of nano-carriers to enhance their applicability in personalized medicine. Overall, our study paves the way for more effective and patient-friendly treatments, highlighting the importance of continuous innovation in nanomedicine.

REFERENCES

- 1. Abdelbary AA, Abd-Elsalam WH, Al-Mahallawi AM. Fabrication of novel ultradeformable bilosomes for enhanced ocular delivery of terconazole: in vitro characterization, ex vivo permeation and in vivo safety assessment. International journal of pharmaceutics. 2016 Nov 20;513(1-2):688-96. https://doi.org/10.1016/j.ijpharm.2016.10.006
- 2. Shukla A, Mishra V, Kesharwani P. Bilosomes in the context of oral immunization: development, challenges and opportunities. Drug discovery today. 2016 Jun 1;21(6):888-99. https://doi.org/10.1016/j.ijpharm.2016.10.006
- 3. Conacher M, Alexander J, Brewer JM. Oral immunisation with peptide and protein antigens by formulation in lipid vesicles incorporating bile salts (bilosomes). Vaccine. 2001 Apr 6;19(20-22):2965-74. https://doi.org/10.1016/S0264-410X(00)00537-5
- 4. Wilkhu JS, McNeil SE, Anderson DE, Perrie Y. Characterization and optimization of bilosomes for oral vaccine delivery. Journal of drug targeting. 2013 Apr 1;21(3):291-9. https://doi.org/10.3109/1061186X.2012.747528
- 5. Pavlović N, Goločorbin-Kon S, Đanić M, Stanimirov B, Al-Salami H, Stankov K, Mikov M. Bile acids and their derivatives as potential modifiers of drug release and pharmacokinetic profiles. Frontiers in Pharmacology. 2018 Nov 8;9:1283. https://doi.org/10.3389/fphar.2018.01283
- 6. Niu M, Lu Y, Hovgaard L, Guan P, Tan Y, Lian R, Qi J, Wu W. Hypoglycemic activity and oral bioavailability of insulin-loaded liposomes containing bile salts in rats: the effect of cholate type, particle size and administered dose. European journal of pharmaceutics and biopharmaceutics. 2012 Jun 1;81(2):265-72. https://doi.org/10.1016/j.ejpb.2012.02.009
- 7. Aburahma MH. Bile salts-containing vesicles: promising pharmaceutical carriers for oral delivery of poorly water-soluble drugs and peptide/protein-based therapeutics or vaccines. Drug delivery. 2016 Jul 23:23(6):1847-67. https://doi.org/10.3109/10717544.2014.976892
- 8. Kumar GP, Rajeshwarrao P. Nonionic surfactant vesicular systems for effective drug delivery—an overview. Acta pharmaceutica sinica B. 2011 Dec 1;1(4):208-19. https://doi.org/10.1016/j.apsb.2011.09.002
- 9. Uchegbu IF, Vyas SP. Non-ionic surfactant based vesicles (niosomes) in drug delivery. International journal of pharmaceutics. 1998 Oct 15;172(1-2):33-70. https://doi.org/10.1016/S0378-5173(98)00169-0
- 10. Ruckmani K, Sankar V. Formulation and optimization of zidovudine niosomes. Aaps Pharmscitech. 2010 Sep;11:1119-27. https://doi.org/10.1208/s12249-010-9480-2
- 11. Ahmad J, Singhal M, Amin S, Rizwanullah M, Akhter S, Amjad Kamal M, Haider N, Midoux P, Pichon C. Bile salt stabilized vesicles (bilosomes): a novel nano-pharmaceutical design for oral delivery of proteins and peptides. Current pharmaceutical design. 2017 Mar 1;23(11):1575-88. https://doi.org/10.2174/1381612823666170124111142

- 12. Swaika A, Crozier JA, Joseph RW. Vemurafenib: an evidence-based review of its clinical utility in the treatment of metastatic melanoma. Drug design, development and therapy. 2014 Jun 16:775-87. https://doi.org/10.2147/DDDT.S31143
- 13. Chen J, Fang C, Chang C, Wang K, Jin H, Xu T, Hu J, Wu W, Shen E, Zhang K. Ultrasound-propelled liposome circumvention and siRNA silencing reverse BRAF mutation-arised cancer resistance to trametinib. Colloids and Surfaces B: Biointerfaces. 2024 Feb 1;234:113710. https://doi.org/10.1016/j.colsurfb.2023.113710
- 14. Lee JW, Choi J, Choi Y, Kim K, Yang Y, Kim SH, Yoon HY, Kwon IC. Molecularly engineered siRNA conjugates for tumor-targeted RNAi therapy. Journal of Controlled Release. 2022 Nov 1;351:713-26. https://doi.org/10.1016/j.jconrel.2022.09.040
- 15. Li W, Zhang H, Assaraf YG, Zhao K, Xu X, Xie J, Yang DH, Chen ZS. Overcoming ABC transporter-mediated multidrug resistance: Molecular mechanisms and novel therapeutic drug strategies. Drug Resistance Updates. 2016 Jul 1;27:14-29. https://doi.org/10.1016/j.drup.2016.05.001